



Imaging with polarized neutrons

M. Strobl^{a,b,*}, N. Kardjilov^b, A. Hilger^b, E. Jericha^c, G. Badurek^c, I. Manke^b

^a University of Heidelberg, Im Neuenheimer Feld 253, 69120 Heidelberg, Germany

^b Helmholtzzentrum Berlin, Glienickerstr. 100, 14109 Berlin, Germany

^c Atominstytut of the Austrian Universities, Stadionalle 2, 1020 Vienna, Austria

ARTICLE INFO

Keywords:

Neutron imaging
Polarized neutrons
Imaging magnetic fields
Polarimetric imaging

ABSTRACT

While polarized neutrons have long proved to be an outstanding tool for the investigation of magnetic structures by scattering, we report on their potential for real space investigations of magnetic fields on a macroscopic scale by neutron imaging. Due to the ability of neutrons to penetrate thick layers of matter and their high sensitivity to magnetic fields owed to their magnetic moment, neutron imaging enables the investigation of magnetic fields even in bulk samples of condensed matter. We demonstrate how neutrons provide images of magnetic fields trapped in or expelled by superconductors or even reveal the path of electric currents due to the corresponding magnetic fields.

© 2009 Elsevier B.V. All rights reserved.

1. Introduction

Neutron imaging has seen a rapid development within the last decade after digital imaging detectors could be employed for recording projection images with high resolution on reasonable time scales [1]. Since then a number of technical [2,3] as well as methodical [4–9] improvements and innovations could be achieved conveying increased spatial and temporal resolution, energy resolved imaging involving Bragg scattering, phase contrast and dark field contrast exploiting the refractive index, respectively, small angle scattering as imaging signals. These developments increased the scope and number of applications in various fields of science and engineering significantly.

Polarized neutrons, however, have been used or proposed for spatially resolved investigations of magnetic fields even before the above developments took place [10–13]. Neutron interferometers as well as double crystal diffractometers provided images of magnetic fields and domain structures in ferromagnetic crystals. The image contrast was introduced by the spin dependent interaction of the neutrons with a magnetic field B due to the corresponding real part of the refractive index $\delta_\mu = \pm \mu B m \lambda^2 / h^2$, where λ is the wavelength, μ the magnetic moment and m the mass of the neutron. However, these instruments work with low intensity beams optimized for high phase, respectively, angular resolution which limits imaging investigations significantly. A recently developed method using a grating based shearing interferometer [6] that can be implemented to state of the art

imaging set-ups might offer the possibility to use the phase signal more efficiently for imaging magnetic fields and structures [14].

An alternative approach is to equip a dedicated imaging facility with a polarizer and a polarization analyzer. In this case the image $I(x, z)$ recorded behind the analyzer is the product of the conventional sample transmission image $I_a(x, z)$ defined by the attenuation law

$$I_a(x, z) = I_0(x, z) e^{-\int \Sigma(x, y, z) dy} \quad (1)$$

with Σ being the linear attenuation coefficient, and the spin phase φ dependent transmission of the analyzer

$$I(x, z) = I_a(x, z) \frac{1}{2} (1 + \cos \varphi(x, z)) \quad (2)$$

According to the well-known Larmor precession of the spin, respectively, magnetic moment of a neutron in an external magnetic field B also the spin phase can be described by a path integral

$$\varphi(x, z) = \frac{\gamma \lambda m}{2\pi \hbar} \int B(x, y, z) dz \quad (3)$$

with γ being the gyromagnetic ratio. Consequently a magnetic field in and around a sample causes additional image contrast due to a signal varying with the cosine of the field integral which is superposing the attenuation image.

2. Measurements and results

Corresponding experiments have been performed at the cold neutron radiography facility CONRAD [15] at the BERII reactor of the Berlin Neutron Scattering Center (BENSNC) of the Helmholtz Center Berlin. Because the precession is dependent on the

* Corresponding author at: University of Heidelberg, Im Neuenheimer Feld 253, 69120 Heidelberg, Germany. Tel.: +49 30 80622490; fax: +49 30 80623094.

E-mail address: strobl@helmholtz-berlin.de (M. Strobl).

wavelength (Eq. (3)) the available double monochromator at CONRAD [9] was used to select a wavelength of 3.5 \AA which corresponds with the maximum of the provided spectrum in the instrument. Solid state polarizing benders [16] have been used to polarize and analyze the beam before, respectively, behind the

sample. The achieved polarization was measured to be approximately 95%.

Different samples have been placed in the beam and some results are presented in the Figs. 1–3. The image sequence in Fig. 1 was recorded observing the Meissner effect after cooling an YBCO

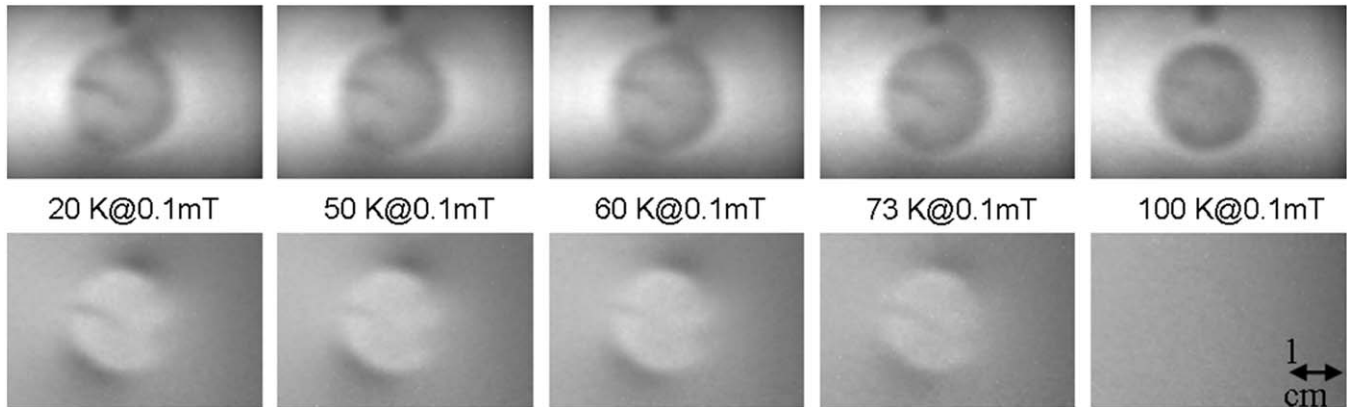


Fig. 1. Radiographic polarized neutron images of an $\text{YBa}_2\text{Cu}_3\text{O}_{7-x}$ (YBCO) superconductor pellet visualizing the Meissner effect; Upper row: raw images; lower row: normalized to attenuation image.

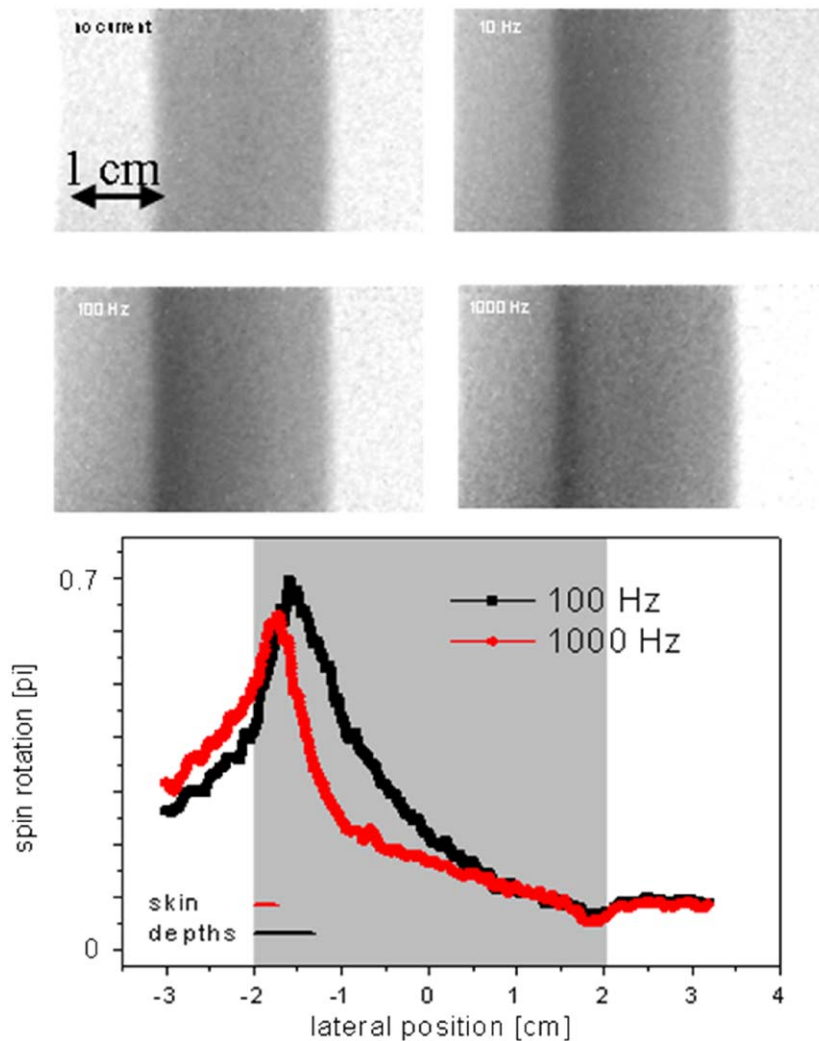


Fig. 2. Radiographies of an Al cylinder with 2 cm diameter contacted asymmetrically to alternating current of different frequencies; the graph shows line profiles of the signal due to the magnetic field achieved by normalization which correspond well to calculated skin depths for the electrical current.

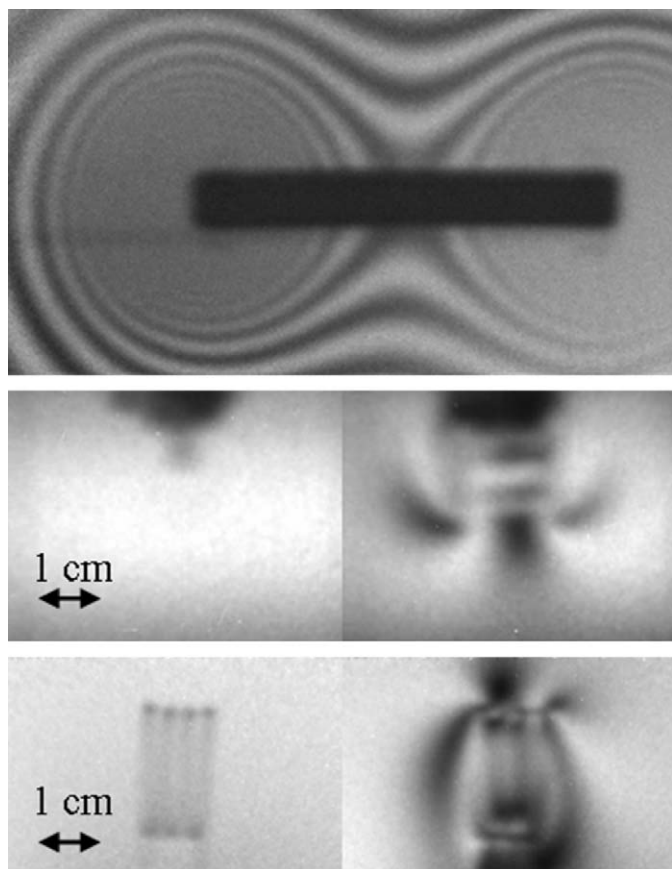


Fig. 3. Polarized neutron images of a permanent dipole magnet (top), a hollow Pb cylinder of 11 mm diameter without (invisible)(left) and with (right) trapped magnetic field (middle) and an electrical coil (diameter 2.5 cm) without (left) and with (right) applied current (bottom).

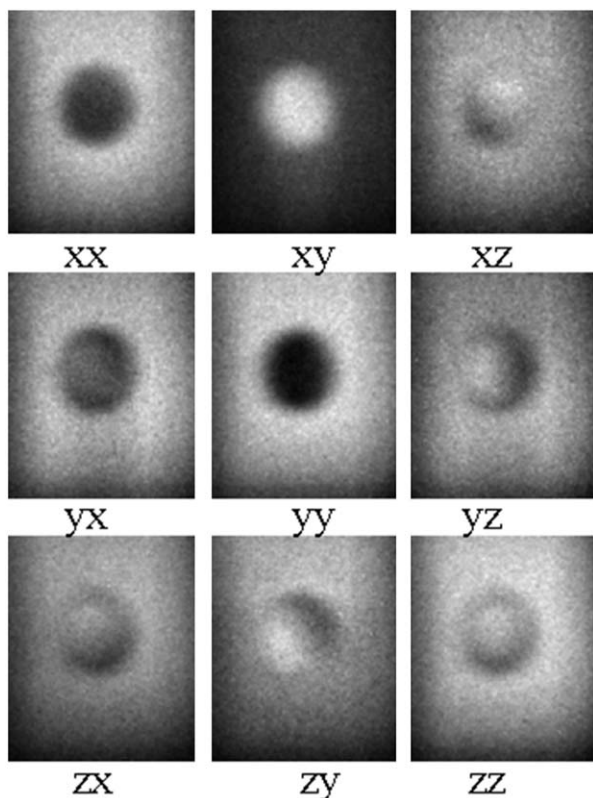


Fig. 4. Polarimetric polarized neutron radiographies of an electrical coil.

pellet down under the critical temperature $T_c = 90$ K. A homogeneous magnetic field perpendicular to the beam and the vertical polarization direction of the neutrons has been produced by a pair of Helmholtz coils. The images in the upper line correspond to the originally achieved images $I(x, z)$ where the attenuation and polarization signal are superposed while below the signal induced by the magnetic field only is represented due to the image normalization

$$I_m(x, z) = \frac{1}{2}(1 + \cos \varphi(x, z)) = I(x, z)/I_0(x, z) \quad (4)$$

with the attenuation image recorded of the pellet without magnetic field. An additional inhomogeneity of the magnetic field expelled from the YBCO due to its superconductivity can be found in the image related to the irregular surface of the pellet. In the case of a cylindrical lead tube a trapped residual field could be found when switching of the magnetic field in which the sample was cooled below $T_c = 7.2$ K (Fig. 3).

Another sample exposed to the polarized beam was an asymmetrically contacted Al cylinder conducting an alternating current. Like shown in Fig. 2 the electrical current could be detected due to the magnetic field it induced. This way the Skin effect and the typical increase of the effect with increasing frequencies could be observed [17].

Additionally it could be demonstrated that under certain conditions involving regular and well aligned field distributions quantitative results can be achieved and even tomographies resulting in volumetric data of a magnetic field can be performed [18]. However, the images in Fig. 3 were chosen in order to also review preliminary limitations of the presented straightforward approach with the given set-up.

Fig. 3 displays three examples of measurements. The image of a dipole magnet is shown in Fig. 3a while images of a cylindrical lead tube with and without a trapped residual magnetic field are displayed in Fig. 3b and c as well as a coil with and without applied electrical current in d and e. All images reveal a relaxed spatial resolution (app. 0.5 mm) compared to the state of the art of approximately $50 \mu\text{m}$ [2]. This is on the one hand due to an increased sample detector distance caused by the polarization analyzer and underlining the need of a compact analyzer. On the other hand the used solid state bender before the sample increases the beam divergence in front of the sample which can easily be avoided by installing a polarizer (bender, polarizing guide) before the collimation path equipped with a guide field or alternatively a polarizer with a bigger cross section but without influence on the divergence (cavity, He3 cell) close to the sample. In Fig. 3a an annular structure related to several spin rotations and the cosine periodicity of Eq. (3) can be found but disappears close to the poles due to the limited spatial resolution. The periodicity complicates, respectively, hinders quantification. However, e.g. the use of different neutron wavelengths and the according shift of the fringes can solve this problem. Furthermore, although the latter samples allow for normalization corresponding to Eq. (4) by the images without magnetic field (compare also Figs. 1 and 2), this is not possible e.g. for the permanent magnet (Fig. 3a). Using a π flipper in front of the sample and the relation of the image achieved with initial spin up and spin down polarization helps to reveal the magnetic signal despite of the beam attenuation. Another challenge is to reveal the full magnetic vector field for irregular fields like in Fig. 3c and e. To achieve the necessary data polarimetric imaging experiments have to be performed in order to record an image for all polarization matrix elements i.e. the measurement of the final polarization direction (P_x, P_y, P_z) for three initial polarization vectors ($P_{0x}, 0, 0$), ($0, P_{0y}, 0$) and ($0, 0, P_{0z}$). Two crossed $\pi/2$ flippers are necessary before and behind the sample. The images of the corresponding nine matrix elements of an electrical coil are presented in Fig. 4.

3. Conclusion

Polarized neutron imaging has the potential to be a powerful tool to investigate magnetic fields even within the bulk of massive samples. This has been demonstrated with several reference samples. Additionally needs for technical and methodical improvements in order to meet the challenges of a wide range of applications have been identified and possible solutions could be named and have been tested.

References

- [1] B. Schillinger, Ph.D. Thesis, TU-München, 1999.
- [2] E. Lehmann, et al., NIMA 576 (2–3) (2007) 389.
- [3] B. Schillinger, J. Brunner, E. Calzada, Phys. B 385–386 (2) (2006) 921.
- [4] B.E. Allman, et al., Nature 408 (2000) 158.
- [5] N. Kardjilov, et al., NIMA 527 (2004) 519.
- [6] F. Pfeiffer, et al., Phys. Rev. Lett. 96 (2006) 215505.
- [7] M. Strobl, et al., Phys. Rev. Lett. 101 (2008) 123902.
- [8] W. Kockelmann, et al., NIMA 578 (2) (2007) 421.
- [9] W. Treimer, et al., Appl. Phys. Lett. 89 (2006) 203504.
- [10] M. Schlenker, et al., J. Magn. Magn. Mater. 15 (8) (1980) 1507.
- [11] K.M. Podurets, R.R. Chistyakov, S.Sh. Shil'shtein, Zh. Tekh. Fiz. 67 (1994) 134.
- [12] G. Badurek, et al., Phys. B 241–243 (1998) 1207.
- [13] M. Strobl, et al., Appl. Phys. Lett. 91 (2007) 254104.
- [14] Ch. Grünzweig, et al., Appl. Phys. Lett. 93 (2008) 112504.
- [15] A. Hilger, et al., Physica B 385–386 (2) (2006) 1213.
- [16] Th. Krist, et al., Physica B 241–243 (1998) 82.
- [17] I. Manke, et al., J. Appl. Phys. 104 (1) (2008) 1.
- [18] N. Kardjilov, et al., Nat. Phys. 4 (2008).